SPAC: Sparse Sensor Placement Based Adaptive Control for High Precision Fuselage Assembly

Shancong Mou, Michael Biehler, Xiaowei Yue, Jeffrey H. Hunt & Jianjun Shi

SPAC: Sparse Sensor Placement Based Adaptive Control for High Precision Fuselage Assembly

Shancong Mou[a], Michael Biehler[a], Xiaowei Yue[b*], Jeffrey H. Hunt[c], and Jianjun Shi[a]

[a]*H. Milton Stewart School of Industrial and Systems Engineering, Georgia Institute of Technology, Atlanta, GA, USA.*

[b]*Grado Department of Industrial and Systems Engineering, Virginia Polytechnic Institute and State University, Blacksburg, VA, USA.*

[c]*The Boeing Company, El Segundo, CA, USA.*

Abstract

Optimal shape control is important in fuselage assembly processes. To achieve high precision assembly, shape adjustment is necessary for fuselages with initial shape deviations. The state-of-the-art methods accomplish this goal by using actuators whose forces are derived from a model based on the designed fuselage mechanical property. This has a significant limitation: they do not consider the model mismatch due to mechanical property changes induced by the shape deviation of an individual incoming fuselage. The model mismatch will result in control performance deterioration. To improve the performance, the shape control model needs to be updated based on the online feedback information from the fuselage shape adjustment. However, due to the large size of the fuselage surface, highly accurate inline measurements are expensive or even infeasible to obtain in practice. To resolve those issues, this paper proposes a Sparse sensor Placement based Adaptive Control (SPAC) methodology. In this method, the model is updated based on the sparse sensor measurement of the response signal. The reconstruction performance under a minor model mismatch is quantified theoretically. Its performance has been evaluated based on real data of a half-to-half fuselage assembly process, and the proposed method improves the control performance with acceptable sensing effort.

Keywords: adaptive control; composite fuselage assembly; sparse sensor placement; quality improvement.

1. Introduction

Composite materials are widely used in the aerospace industry due to their superior chemical and mechanical properties (Clyne and Hull 2019). In the assembly process, multiple composite fuselages need to be assembled with high precision. However, shape deviations during the fabrication and transportation lead to inevitable dimensional variability of composite fuselages (Yue et al. 2018). This

dimensional variability can cause large gaps between subassemblies. Without appropriate compensation, it will cause a significant increase in the flowtime, manpower cost and even halt the delivery of the airplane (Duncan 2021). For a detailed discussion on the assembly process, we refer interested readers to Manohar et al. (2018b). To overcome this issue, aircraft assemblers use actuators to adjust the edges of the fuselage to their target shape for reducing the gap. An illustrative figure of a half fuselage is shown in Figure 1. In practice, the force applied by each actuator is determined by a trial-and-error approach, which is inefficient, sub-optimal, and requires highly experienced engineers.
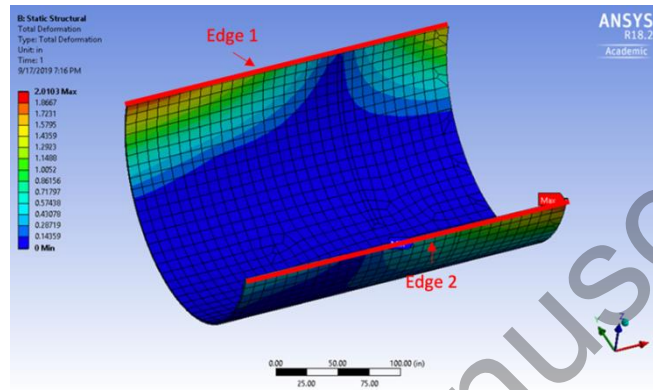

Figure 1. Illustration of a half fuselage

To achieve better dimensional control of the fuselage, an automatic optimal shape control (AOSC) of fuselages was proposed to determine the actuators' forces and locations (Yue et al. 2018). Since then, multiple methods for modeling and optimal shape control of fuselages have been proposed (Wen et al. 2018, Yue et al. 2018, Du et al. 2019, Zhong et al. 2021). These control strategies can be separated into two categories in terms of different modeling approaches: (i) first-principle-based methods (Zhang and Shi 2016a, Zhang and Shi 2016b, Wen et al. 2018, Zhong et al. 2021), and (ii) data-driven methods (Yue et al. 2018, Yue and Shi 2018, Du et al. 2019, Lee et al. 2022). For first-principle-based methods, Wen et al. (2018) built a finite element analysis (FEA) model to mimic the physical properties of a fuselage. Zhang and Shi (2016a,b) proposed a stream of variation model for compliant parts. Furthermore, Zhong et al. (2021) proposed an FEA model-based control strategy and incorporated the cautious control concept to consider part-to-part uncertainties. For data-driven methods, Yue et al. (2018) proposed a surrogate model-based control framework that considers uncertainties for the fuselage assembly. Du et al. (2019) proposed a sparse-learning framework to

select the actuator locations and forces automatically. Lee et al. (2022) developed the neural network Gaussian process considering input uncertainty, and achieved accurate predictions. Wang et al. investigated the theoretical performance of Gaussian processes with input uncertainties. The main drawbacks of those existing methods are twofold:

(i) For the first-principle-based methods, it is time-consuming and challenging to build an accurate model for each incoming fuselage due to the inherent production variation. Usually, the model is built according to the designed shape and materials. Therefore, it does not represent an individual incoming fuselage accurately.

(ii) Data-driven methods are built upon the experimental data of real fuselages or FEA simulations. This can be considered as a population model for fuselages. However, accurately measuring the thickness, material property, or fastening conditions for each incoming fuselage is complicated. Therefore, these models may fail to predict the outputs accurately when the response surface goes beyond the scope of experimental data.

Furthermore, all the aforementioned methods are one-shot methods, i.e., no feedback information is used to update the model so that the unique characteristics of an incoming part can be considered. This will lead to a mismatch between the physical model of the incoming fuselage and the model used to derive the control strategy. Even though the model mismatch may be small, the derived control strategy will lead to suboptimal control performance, which is undesirable due to the ultra-high precision requirement for the composite fuselage assembly.

Adaptive control methods can update the model accurately with the help of online estimation using feedback information and derive a control strategy fitting the specific incoming fuselage (Landau et al. 2011). It is widely used in the control of dynamic systems with unknown or time-varying parameters (Åström 1983, Landau et al. 2011, Åström and Wittenmark 2013). Adaptive control methods can be summarized into three categories: open-loop adaptive control, direct adaptive control, and indirect adaptive control methods (Landau et al. 2011). Among these methods, the indirect adaptive control is closely related to the fuselage assembly process, where the model of the fuselage can be estimated online from the input-output measurements, and the control action can be

3

determined accordingly. The indirect adaptive control method includes two stages: (i) online model parameter estimation and (ii) online computation of the controller parameters. Traditionally, existing parameter adaptation algorithms, such as Gradient Descent or Least-Squares Minimization, can achieve satisfactory parameter estimation based on the feedback information when the response signal has a low dimension. However, the fuselage has a large surface area (e.g., Section 41 fuselage of Boeing 787 is 6.2 meters in diameter and 12.8 meters long (Sloan 2018)). High precision measurement of the deformation of the fuselage usually generates high-dimensional signals (e.g., as shown in Figure 1, the 186 measurements correspond to the 62 grid points on two edges, each grid point requiring 3-dimensional measurement leading to a 186-dimensional signal in our case study). Acquiring such accurate high dimensional feedback information in a fuselage assembly requires many repetitive measurements, resulting in significant cost increase and production delay. Therefore, the trade-off between control performance and measurement cost needs to be considered.

To reduce the sensing cost, sparse sensor placement has been widely used in the field of signal processing (Donoho 2006, Candès and Wakin 2008, Joshi and Boyd 2008) and control (Manohar et al. 2018a). The main idea of the sparse sensor placement is to reconstruct the response signal with a small subset of samples. Current approaches for sparse sensor placement commonly utilize a brute-force, combinatorial search, which is computationally intractable even for moderately large systems (Brunton et al. 2016). By exploiting structural properties such as low rank (Manohar et al. 2018a, Manohar et al. 2018b) or sparsity (Candès and Wakin 2008), the sparse sensor placement problem can be solved efficiently (Brunton et al. 2016). Sparse sensor placement has been applied in a large number of real-world applications involving signal compression (Candès and Wakin 2008), environmental monitoring of ocean temperatures (Yang et al. 2010), structural health monitoring (Meo and Zumpano 2005), and dynamical systems (Kramer et al. 2017). The sensing cost can be significantly reduced by adopting the sparse sensor placement strategy while maintaining comparable measurement accuracy requirements.

There are generally two types of sparse sensor placement methods (Manohar et al. 2018a): (i) One is based on the sparse representation of the sensing signal, also called compressive sensing

(Candès and Wakin 2008). Compressive sensing aims to reconstruct the entire signal based on a small number of measurements. The sensors are usually randomly placed, and the reconstruction leads to an l_1 norm minimization problem. (ii) The other is based on the low-rank representation of the sensing signal in a low-dimensional subspace. The basis spanning this subspace is also called tailored basis. To optimize the sensor location in this case, a regression problem has to be solved, and usually experimental design concepts are utilized. In terms of using sparsity to reduce the sensing cost, Bhattacharya and Başar (2011) proposed using compressive sensing techniques to provide feedback information in controlling the system. However, the second category is more suitable for fuselage assembly problems because

(i) it is infeasible or time-consuming to place sensors randomly (Manohar et al. 2018a).

(ii) under the small deformation assumption (Reddy 2019, Zhong et al. 2021), the deformation of the fuselage lives in a low dimensional space driven by a small number of actuators, which is low rank rather than sparse (more details refer to Section 2.2).

Therefore, we need to estimate the low-rank space for sparse sensor placement and incorporate the impacts of the physical model of the incoming fuselage.

In this paper, we propose a SPAC strategy that utilizes the feedback information for model updating to improve the control performance while keeping the measurement cost at a reasonable level by integrating a sparse sensor placement framework. The main challenge is the unknown physical model during the reconstruction of the response signal from sparse sensor measurement. We propose to use the system equations derived from the design information or learned from historical data as an alternative. The slight mismatch between the physical model of the incoming fuselage and the designed one is called the perturbation to the model. A theoretical quantification of the reconstruction error is derived in this scenario. The corresponding engineering interpretation is given, which may serve as a guideline for determining the number of sensors needed according to the perturbation level. Furthermore, we use a case study in the high precision fuselage assembly process to show that the SPAC framework can achieve comparable control performance as the adaptive control method with much less sensing cost.

The remainder of this paper is organized as follows. Section 2 presents the sparse sensor placement methodology and analyzes its reconstruction performance under small perturbations. In Section 3, the proposed SPAC framework is applied in a high precision fuselage assembly process. Finally, Section 4 concludes the paper.

2. Sparse Sensor Placement based Adaptive Control Methodology

This section proposes the SPAC methodology to address the research gap of integrating the sparse sensor placement in the presence of model perturbation into the adaptive control. Figure 2 provides an overview of the proposed SPAC methodology.
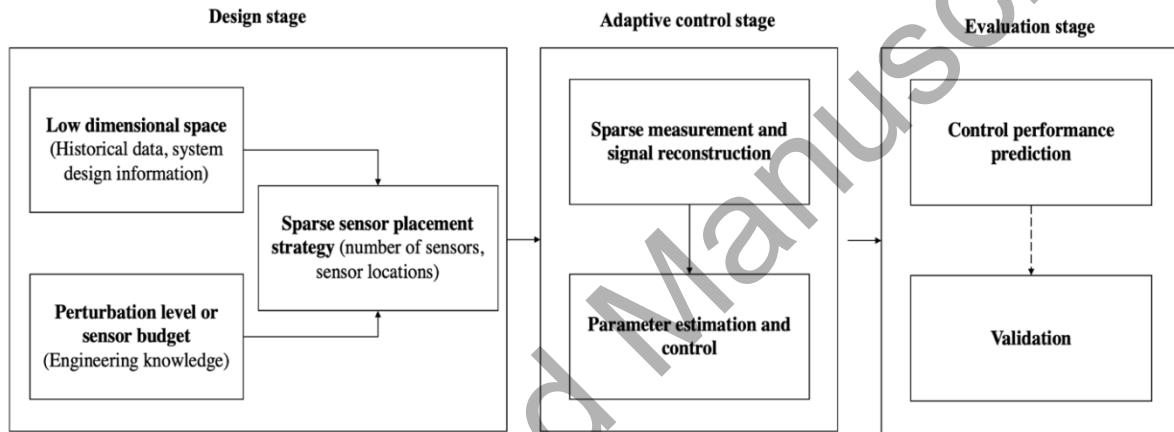

Figure 2. An overview of the proposed SPAC method

The proposed SPAC method has three stages:

(i) In the design stage, a low-dimensional intrinsic space, to which a high-dimensional response signal can be projected without loss of critical information, is derived either based on historical data or the system equation. The sparse sensor placement strategy determines the number of sensors and their corresponding locations by incorporating the perturbation level or sensor budget from engineering knowledge.

(ii) In the adaptive control stage, the entire response signal (e.g., fuselage's high-dimensional shape deviation) is first reconstructed from the sparse measurement signals. Afterward, appropriate algorithms can be applied for parameter estimation and control.

6

(iii) In the evaluation stage, the control performance will be predicted from the sparse measurement signal, and the performance can be validated using the measured dimensional deviation data.

In Section 2.1, a sparse sensor placement strategy is introduced. Then, the reconstruction performance of the proposed method under small perturbations is presented in Section 2.2. Finally, the downstream parameter estimation and adaptive control strategy are proposed.

2.1 Sparse sensor placement methodology

The goal of the sparse sensor placement methodology is to select a subset of sensors from all potential sensor locations to reconstruct the entire measurement field. There are two types of sparse sensor placement strategies:

(i) The first strategy is based on the sparse representation of the sensing signal to sample randomly on a universal encoding basis. This strategy is related to compressive sensing (Candès and Wakin 2008).

(ii) The second strategy is based on the low-rank representation of the sensing signal with a set of known bases that lead to a designed measurement strategy. This type of strategy is closely related to experimental design (Chaloner and Verdinelli 1995).

In the control context, the high-dimensional raw response signal is usually driven by a low-dimensional critical control signal. This indicates that the response usually lives in known, lower-dimensional space. Low-dimensional representation can retain the most meaningful features of the original data. Since the second approach exploits this low-rank structure, it is commonly satisfied in high-dimensional control systems. By adopting this approach, the sensing cost can be significantly reduced.

Let $\boldsymbol{y}_t \in \mathbb{R}^n$ denote the response at time step t of a control signal $\boldsymbol{x}_t \in \mathbb{R}^m$, i.e., $\boldsymbol{y}_t = \mathbf{A}\boldsymbol{x}_t$, where $\mathbf{A}$ is assumed to be of full column rank, $\mathbf{A} \in \mathbb{R}^{n \times m}$ and $m \ll n$. $\boldsymbol{y}_t, \forall t \in \{1,2,3 \dots\}$, can be projected into a low-dimensional space spanned by column space of $\mathbf{A}$. We can reconstruct $\boldsymbol{y}_t$ with only m measurement points when there is no measurement noise. For robustness, we propose to use p measurement points out of n potential locations where $p \in \{m, m + 1, \dots, n\}$. For ease of exposition,

we will suppress the subscript t in the following discussion. Let sensor locations be $\Gamma = \{\gamma_1, \ldots, \gamma_p\} \subseteq$ $\{1, \ldots, n\}$ and $\boldsymbol{y}' = \left[y_{\gamma_1}, \ldots, y_{\gamma_p}\right]^{\mathrm{T}}$ be the sparse measurement. Let $\mathbf{C} = \left[\boldsymbol{e}_{\gamma_1}, \ldots, \boldsymbol{e}_{\gamma_p}\right]^T$ be the selection matrix, where $\boldsymbol{e}_{\gamma_i}$ (i=1, 2, …, p) is a unit vector with all zeros except for a unit element on location γ_i, i.e.,

$$\boldsymbol{y}' = \mathbf{C}\boldsymbol{y} + \boldsymbol{\epsilon}, \#(1)$$

where $\boldsymbol{\epsilon}$ is the measurement error that follows a multivariate Gaussian distribution, i.e., $\boldsymbol{\epsilon} \sim N\left(\mathbf{0}, \sigma^2 \boldsymbol{I}_p\right)$.

The high-dimensional response $\boldsymbol{y}$ can be written as a linear combination of the column vectors of $\mathbf{A}$, i.e., $\boldsymbol{y} = \sum_i^m A(:,i)x_i$, where $A(:,i)$ is the ith column vector of matrix $\mathbf{A}$. Substituting this relationship in Eq. (1), we obtain

$$\boldsymbol{y}' = \mathbf{C}\mathbf{A}\boldsymbol{x} + \boldsymbol{\epsilon}. \#(2)$$

Once $\boldsymbol{y}'$ is measured, and $\mathbf{C}\mathbf{A}$ is known, $\boldsymbol{x}$ can be estimated as $\hat{\boldsymbol{x}} = (\mathbf{C}\mathbf{A})^{\dagger}\boldsymbol{y}'$, where $(\mathbf{C}\mathbf{A})^{\dagger} = [(\mathbf{C}\mathbf{A})^{\mathrm{T}}\mathbf{C}\mathbf{A}]^{-1}(\mathbf{C}\mathbf{A})^{\mathrm{T}}$. The estimation error $\hat{\boldsymbol{x}} - \boldsymbol{x}$ has zero mean and covariance $\boldsymbol{\Sigma} = \sigma^2[(\mathbf{C}\mathbf{A})^{\mathrm{T}}\mathbf{C}\mathbf{A}]^{-1}$. There are several commonly used optimization criteria for sensor placement or optimal experimental design (Chaloner and Verdinelli 1995), which are summarized as follows:

(i)   Spectral radius criterion (E-optimality):

$$\Gamma = \mathrm{argmin}_{|\Gamma|=p}\left\|[(\mathbf{C}\mathbf{A})^{\mathrm{T}}\mathbf{C}\mathbf{A}]^{-1}\right\|_2 = \mathrm{argmax}_{|\Gamma|=p}\sigma_{min}, \#(3)$$

where σ_{min} is the minimum singular value of $\mathbf{C}\mathbf{A}$.

(ii) Trace criterion (A-optimality):

$$\Gamma = \mathrm{argmax}_{|\Gamma|=p}\mathrm{tr}\left([(\mathbf{C}\mathbf{A})^{\mathrm{T}}\mathbf{C}\mathbf{A}]^{-1}\right), \#(4)$$

where $\mathrm{tr}(\mathbf{M})$ is the trace of matrix $\mathbf{M}$.

(iii) Determinant criterion (D-optimality):

$$\Gamma = \mathrm{argmax}_{|\Gamma|=p}\mathrm{det}\left((\mathbf{C}\mathbf{A})^{\mathrm{T}}\mathbf{C}\mathbf{A}\right), \#(5)$$

where $\mathrm{det}(\mathbf{M})$ is the determinant of matrix $\mathbf{M}$.

These three criteria have different statistical interpretations: the E-optimality criterion maximizes the minimum eigenvalue of the information matrix; the A-optimality can minimize the

summation of marginal variances for x; while the D-optimality maximizes the confidence region volume for parameters x. The choice of those criteria is usually based on specific problem requirements. In the following discussion, we will focus on the determinant criterion, which is widely used in sparse sensor placement (Joshi and Boyd 2008, Manohar et al. 2018a, Manohar et al. 2018b).

2.2 Reconstruction performance under small perturbations

In this section, we will derive the reconstruction performance under small perturbations. As mentioned in Section 2.1, **A** is necessary for deriving a sparse sensor placement strategy, which can be derived from the system model. However, the real system model may deviate from the system equations obtained from the engineering design (or from historical data). For example, in the automatic control for fuselage assembly, the system model is given by finite element analysis (Wen et al. 2018) or experimental design (Yue et al. 2018, Du et al. 2019), which is not the same as the system equation of incoming fuselages due to initial shape deviations. Meanwhile, it is not feasible to model every incoming fuselage individually. Therefore, we propose to use $\mathbf{A}_0$ from the designed system model to derive the sparse sensor placement strategy. In this case, the reconstruction performance of the sparse sensor placement under small perturbations needs to be quantified. Furthermore, the influence of the parameter estimation and control of this perturbed high-dimensional system needs to be studied.

In the following discussions, we will use an l_2 norm perturbation. The induced l_2 norm of any matrix $\mathbf{M} \in \mathbb{R}^{m \times n}$ is defined as $\|\mathbf{M}\|_2 = \max_{\|x\|_2 \leq 1, x \in \mathbb{R}^m} \|\mathbf{M}x\|_2$. The induced l_2 norm of a matrix $\mathbf{A}$ is also its spectral norm, which equals the largest singular value of $\mathbf{A}$. We use $\mathbf{A}_0$ as the matrix derived from engineering design which is also the one we observed (*designed matrix*), and $\mathbf{A}$ as the normalized true matrix derived from the system model of an incoming fuselage with initial shape deviation, which is the *perturbed matrix* from the designed one. We are interested in the reconstruction performance under a small l_2 perturbation, i.e., $\|\mathbf{\Delta}\|_2 = \|\mathbf{A} - \mathbf{A}_0\|_2 \leq \delta$ is small. δ is defined as the perturbation level.

9

Let $\widehat{\boldsymbol{y}}_0$ be the reconstructed signal which is estimated by using $\mathbf{A}_0$ and the measured signal $\boldsymbol{y}'$, i.e.,

$$\widehat{\boldsymbol{y}}_0 = \mathbf{A}_0\widehat{\boldsymbol{x}} = \mathbf{A}_0(\mathbf{C}\mathbf{A}_0)^{\dagger}\boldsymbol{y}' \#(6)$$

The distribution of the reconstruction error $\widehat{\boldsymbol{y}}_0 - \boldsymbol{y}$ is presented in the following proposition.

Proposition 1. Let $\mathbf{A} \in \mathbb{R}^{n \times m}$ be the perturbed matrix and $\boldsymbol{\Phi}_0 \in \mathbb{R}^{n \times m}$ be the designed matrix. Let $\boldsymbol{\Delta} = \mathbf{A} - \mathbf{A}_0$ be the perturbation bounded by δ, i.e., $\|\boldsymbol{\Delta}\|_2 \leq \delta$. Let $\mathbf{C}_0 \in \mathbb{R}^{p \times n}$ and $\mathbf{C} \in \mathbb{R}^{p \times n}$ be the selection matrix that solves one of the Equations (3-5) using $\mathbf{A}_0$ and $\mathbf{A}$, respectively. Assume that the perturbation $\boldsymbol{\Delta}$ is small such that the selection matrix $\mathbf{C}_0 = \mathbf{C}$, and $\mathbf{C}_0\mathbf{A}_0 \in \mathbb{R}^{p \times m}$ is of full column rank. Let $\widehat{\boldsymbol{y}}_0 = \mathbf{A}_0(\mathbf{C}\mathbf{A}_0)^{\dagger}\boldsymbol{y}'$, where $\boldsymbol{y}'$ is the measured signal subjecting to measurement error $\boldsymbol{\epsilon} \sim N(\mathbf{0}, \sigma^2 \boldsymbol{I}_p)$, i.e., $\boldsymbol{y}' = \mathbf{C}\mathbf{A}\boldsymbol{x} + \boldsymbol{\epsilon}$, where $\boldsymbol{x}$ is the input control signal. Then the reconstruction error $\widehat{\boldsymbol{y}}_0 - \boldsymbol{y}$ also follows a multivariate Gaussian distribution with mean $\boldsymbol{\mu}_1$ and covariance $\boldsymbol{\Sigma}_1$, i.e., $\widehat{\boldsymbol{y}}_0 - \boldsymbol{y}' \sim N(\boldsymbol{\mu}_1, \boldsymbol{\Sigma}_1)$, such that

$$\boldsymbol{\mu}_1 = \mathbf{A}_0(\mathbf{C}_0\mathbf{A}_0)^{\dagger}\mathbf{C}\mathbf{A}\boldsymbol{x} - \mathbf{A}\boldsymbol{x}, \#(7)$$

$$\boldsymbol{\Sigma}_1 = \sigma^2 \mathbf{A}_0[(\mathbf{C}_0\mathbf{A}_0)^{\mathrm{T}}\mathbf{C}_0\mathbf{A}_0]^{-1}(\mathbf{A}_0)^{\mathrm{T}}. \#(8)$$

Moreover,

$$\|\boldsymbol{\mu}_1\|_2 \leq \left\|\mathbf{A}_0(\mathbf{C}_0\mathbf{A}_0)^{\dagger}\mathbf{C}_0 - \mathbf{I}\right\|_2 \|\boldsymbol{x}\|_2 \delta, \#(9)$$

and with a probability at least $\left(1 - \frac{\sigma^2}{(\|\mathbf{C}\mathbf{A}\boldsymbol{x}\|_2/p)^2}\right)$,

$$\|\widehat{\boldsymbol{y}}_0 - \boldsymbol{y}\|_2 \leq \left\|\mathbf{A}_0(\mathbf{C}_0\mathbf{A}_0)^{\dagger}\mathbf{C}_0 - \mathbf{I}\right\|_2 \|\boldsymbol{x}\|_2 \delta + \left\|\mathbf{A}_0(\mathbf{C}_0\mathbf{A}_0)^{\dagger}\right\|_2 \|\mathbf{C}\mathbf{A}\boldsymbol{x}\|_2. \#(10)$$

The proof for Proposition 1 is provided in Appendix A.

Discussion of Proposition 1

Proposition 1 shows that $\widehat{\boldsymbol{y}}_0$ is no longer an unbiased estimator of $\boldsymbol{y}$ if there is a perturbation to the basis. However, the bias can be bounded tightly if the induced perturbation is small in terms of the l_2-norm. The following discussions give the engineering interpretation of this proposition.

(i) The probability $\left(1 - \frac{\sigma^2}{(\|\mathbf{C}\mathbf{A}\boldsymbol{x}\|_2/p)^2}\right)$ is dominated by the signal-to-noise ratio $\frac{\|\mathbf{C}\mathbf{A}\boldsymbol{x}\|_2/p}{\sigma}$. The higher the signal-to-noise ratio is, the more the estimation error $\widehat{\boldsymbol{y}}_0 - \boldsymbol{y}$ will concentrate to an

l_2 ball with center $\boldsymbol{\mu}_1$. Therefore, the reconstruction error will be bounded with a higher probability when the signal-to-noise ratio is high.

(ii) Notice that there are two terms in $\|\widehat{\boldsymbol{y}}_0 - \boldsymbol{y}\|_2$: the first term is the bias $\boldsymbol{\mu}_1$ due to the perturbation and dominated by the perturbation magnitude δ. Therefore, intuitively a smaller perturbation will also lead to a better reconstruction performance. The second term is necessary due to measurement errors, which will have a significant influence on the reconstruction performance, especially when the signal-to-noise ratio is low.

2.3 Adaptive control of the perturbed system with sparse sensor measurements

In this section, we will discuss the proposed control strategy. The goal is to estimate $\mathbf{A}$ and solve for the optimal control action that can achieve the control goal. Assume that the matrix $\mathbf{A}_0 \in \mathbb{R}^{n \times m}$ are derived from engineering design and the perturbation level δ are known.

Suppose a set of control signals $\mathbf{X} = [\boldsymbol{x}_1, \dots, \boldsymbol{x}_N] \in \mathbb{R}^{m \times N}$ and the corresponding reconstructed response signals $\widehat{\mathbf{Y}} = [\boldsymbol{y}_1, \dots, \boldsymbol{y}_N] \in \mathbb{R}^{n \times N}$ are collected by sparse measurements, where $N > m$ is the sample size. The sparse sampling and reconstruction are based on the known system matrix $\mathbf{A}_0$.

A common approach in adaptive control is to update the model using the least square method (Landau et al. 2011):

$$\widehat{\mathbf{A}} = \mathrm{argmin}_{\mathbf{A}} \left\| \widehat{\mathbf{Y}} - \mathbf{AX} \right\|_F \#(11)$$

where $\|\cdot\|_F$ is the Frobenius norm.

Assume the control goal is to keep the response close to a target response signal $\boldsymbol{y}_T$, then the control action $\boldsymbol{x}$ can be obtained as follows

$$\widehat{\boldsymbol{x}} = \mathrm{argmin}_{\boldsymbol{x}} L_{\widehat{\mathbf{A}}}(\boldsymbol{y}_T, \boldsymbol{x}) \#(12)$$

where $L_{\widehat{\mathbf{A}}}(\cdot, \cdot)$ is the loss function.

Proposition 2. If the loss function is $L_{\widehat{\mathbf{A}}}(\boldsymbol{y}_T, \boldsymbol{x}) = \left\| \boldsymbol{y}_T - \widehat{\mathbf{A}}\boldsymbol{x} \right\|_2^2$, then the control result of using SPAC by solving (12) with selection matrix $\mathbf{C}$ is

$$\boldsymbol{y}_{ctr} = \mathbf{A}\bigl(\widehat{\mathbf{A}}\bigr)^{\dagger} \boldsymbol{y}_T,$$

where $\widehat{\mathbf{A}}$ is the solution of (11), i.e., $\widehat{\mathbf{A}} = \mathbf{A}_0 (\mathbf{C}\mathbf{A}_0)^{\dagger} \mathbf{Y}' \mathbf{X}^{\mathrm{T}} (\mathbf{X}\mathbf{X}^{\mathrm{T}})^{-1}$.

The proof for Proposition 2 is provided in Appendix B.

Note that there are two sources of control performance loss:

(i)   The *reconstruction error* of the response signal using the designed system matrix $\mathbf{A}_0$. This can be reduced by increasing the number of sensors.

(ii)   The *measurement error*, which can be reduced by using sensors with a higher signal-to-noise ratio.

The number of sensors and sensor accuracy should be determined by the engineers considering the trade-off between control performance requirement and the sensing budget.

The SPAC method for the perturbed system is summarized in Algorithm 1.

Algorithm 1. SPAC method for the perturbed system

Input:

 Sample size N, sensor budget p, known $\mathbf{A}_0$, optimality criterion.

Sparse sensor placement:

Get the sensor selection matrix $\mathbf{C}$ by solving problems (3)-(5) with corresponding criteria.

Adaptive control:

 Sampling and reconstruction:

  collect a set of control signal $\mathbf{X} = [\boldsymbol{x}_1, \dots, \boldsymbol{x}_N] \in \mathbb{R}^{m \times N}$ and the corresponding measurement $\mathbf{Y}' = [\boldsymbol{y}'_1, \dots, \boldsymbol{y}'_N] \in \mathbb{R}^{p \times N}$, calculate the reconstructed response signal using: $\widehat{\mathbf{Y}}_0 = \mathbf{A}_0 (\mathbf{C}\mathbf{A}_0)^{\dagger} \mathbf{Y}'$

 Parameter estimation and control:

  Estimate the system equation by solving (11) and derive the control strategy by solving (12).

---

3. Case Study

This section will validate the proposed SPAC method using the shape control of a high precision composite fuselage assembly process (Yue et al. 2018, Du et al. 2019). In the assembly process of

composite fuselages, there are inherent dimensional variabilities due to the fabrication and transportation of composite parts. Those dimensional variabilities not only cause large gaps in the subassemblies but also lead to perturbations of fuselages' mechanical properties from the designed ones. The perturbation makes the control strategy derived from the designed shape suboptimal.

We propose to use the sensing feedback information to control the fuselage assembly with initial shape deviation. The models from engineering design or learned from historical data are used to derive the sparse sensor placement strategy for fuselages with initial shape deviation. On the one hand, due to the tight engineering specifications in the manufacturing process, the perturbed true model for each incoming fuselage should be close to the designed one, although not identical. This enables us to utilize the designed model to reconstruct the response signal. On the other hand, the dimension of the input control signal (e.g., the number of actuators) in the shape control of fuselage application is much smaller than the dimension of the response (e.g., the deformation of fuselage edges). Therefore, utilizing the sparse sensor placement concept is suitable to reduce sensing costs.

The SPAC control framework for the high precision composite fuselage assembly process is shown in Figure 3. For an incoming fuselage, the sparse learning based automatic optimal shape control (Du et al. 2019) is applied to the fuselage. If the actual control performance and expected control performance are close to each other, no more control action is needed. Otherwise, the SPCA is applied to improve the control performance. Finally, if the control result meets the assembly precision requirement, the fuselage panels will be assembled. Otherwise, shimming is needed.
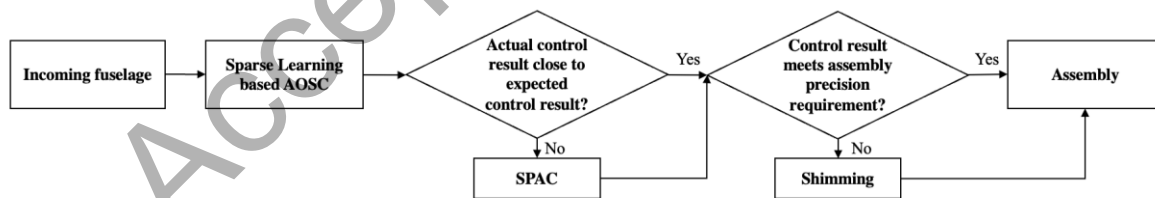

Figure 3. SPAC control framework for high precision composite fuselage assembly process

In Section 3.1, the FEA-based process model is briefly introduced. Then, the control performance of using the adaptive strategy is presented in Section 3.2. The accurate dynamic measurement of the fuselage's high-dimensional shape deviation is expensive, though essential for the

high precision fuselage shape control. Therefore, a good balance between measurement budget and control precision can improve the control performance without a significant cost increase. Consequently, the SPAC approach is adopted in Section 3.3. A comparison study is also conducted to demonstrate the effectiveness of the proposed method.

3.1 FEA-based process model

In this case study, we will adopt the FEA-based process model since it is directly derived from the first principles and has a better engineering interpretation. The proposed method can be applied to both types of modeling approaches. For the detailed description of the FEA-based process model, readers are encouraged to refer to (Zhong et al. 2021).

Let $y \in \mathbb{R}^{n \times 1}$ be the deviation vector of points on the two edges of the fuselage and $f_a \in \mathbb{R}^{n_1 \times 1}$ be the actuator force vector, where n_1 is the total number of degrees of freedom of nodes on the fuselage surface, and n is the total number of degrees of freedom of nodes on the two edges of the fuselage. The system equation can represent the relationship between the mechanical response behavior of nodes on edges and actuator forces as

$$y = \mathbf{B}_1 f_a, \#(13)$$

where $\mathbf{B}_1 \in \mathbb{R}^{n \times n_1}$ is the full rank modified stiffness matrix loaded from the FEA platform (according to design information). The number and locations of actuators are determined by adopting the sparse learning methodology (Du et al. 2019) and solving the following optimization problem:

$$f_a = \underset{f_a}{\text{argmin}} \|y_0 + y - y_T\|_\infty + \lambda \|f_a\|_1, \#(14)$$

Subject to

$$y = B_1 f_a,$$

$$\|f_a\|_\infty \leq \bar{f},$$

where y_T is the target shape and $\bar{f}$ is the upper bound of the allowable force to ensure the safety specifications of the fuselage structure. $\bar{f}$ can be determined by the maximum equivalent stress or failure criteria such as Tsai-Wu, Tsai-Hill, and Hoffman criteria (Jones 1998). The solution to Problem (14), f_a, is a sparse actuator force whose nonzero elements are controlled by the tuning

parameter λ. The nonzero elements can indicate the location of actuators. λ is selected such that the number of nonzero elements in $\boldsymbol{f}_a$ is within the required limit of actuators. Let $\boldsymbol{x} \in \mathbb{R}^m$ be the force vector consisting of nonzero elements in $\boldsymbol{f}_a$ and $\mathbf{B}_2 \in R^{n_1 \times m}$ be the mapping such that $\boldsymbol{f}_a = \mathbf{B}_2 \boldsymbol{x}$.

In the following control process, we will fix the actuator locations ($\mathbf{B}_2$) and only update the actuator forces ($\boldsymbol{x}$). Therefore, the system equation to be updated has the following form:

$$\boldsymbol{y} = \mathbf{B}_1 \mathbf{B}_2 \boldsymbol{x} = \mathbf{A}\boldsymbol{x} \#(15)$$

where $\mathbf{A} = \mathbf{B}_1 \mathbf{B}_2 \in \mathbb{R}^{n \times m}$. Notice that the dimension of $\boldsymbol{x}$ is usually small due to the actuator budget limit. While the response $\boldsymbol{y}$ itself can be high-dimensional, the change of $\boldsymbol{y}$, due to control action $\boldsymbol{x}$, lives in a low-dimensional space spanned by the left singular matrix of $\mathbf{A}$. In the following discussion, we will demonstrate the proposed method using an FEA model built upon a set of parameters validated by Wen et al. (2018). There are 62 points on those two edges, generating a 186-dimensional response signal.

3.2 Control performance of the adaptive strategy

In this section, we will compare the control performance of the proposed SPAC method with the sparse learning method (Du et al. 2019) (one-shot control method) and the regular adaptive control method which measures the whole response signal. We verify that the SPAC method can achieve comparable control performance with the regular adaptive control method but with much less sensing cost.

In practice, there are multiple ways to measure the fuselage shape deviations. Laser Radar (LR) (Muralikrishnan et al. 2016) can achieve high measurement accuracy, but the measurement speed is slow. iGPS can be used to perform dynamic measurements with high data acquisition rate. However, its accuracy is lower than that of LR. Due to the nature of adaptive control, the incoming fuselage can be measured offline before assembly. Therefore, high precision measurement techniques such as LR can be used. During the assembly process, in-situ measurement of the feedback signal is preferred for the adaptive control. Therefore, dynamic measurement techniques such as iGPS need to be adapted. To mimic this process, we generate 19 fuselages with initial shape deviation from FEA in our simulation. During the adaptive control process, we increase the measurement error to reflect the

15

fact of using the dynamic measurement technique, i.e., an i.i.d. Gaussian random noise with mean zero and standard deviation 0.066 mm (Mei and Maropoulos 2014) will be added to each node on top of the FEA simulation result as the measured deviation.

We will first apply the sparse learning method (Du et al. 2019) on 19 incoming fuselages with initial shape deviations. Its control results are the baseline for the comparison study. For SPAC, we adopt the $\|\cdot\|_2$ loss function in Equation (12).

For the sparse learning method, the actuator budget is 20. After the actuator locations are fixed, we solve the control optimization problem to get its best one-shot control performance. As a one-shot control method, the sparse learning control model is derived based on the design information. To evaluate its control performance, we calculate (i) the true control result of applying the derived control strategy on the fuselage with the same initial shape deviation and the corresponding perturbed model; and (ii) the expected control result of applying the derived control strategy on an ideal fuselage with the same initial shape deviation and the designed model. The initial deviation (right-slanted bar), the true control result (crossed bar), and the expected control result (dotted bar) are shown in Figure 4.
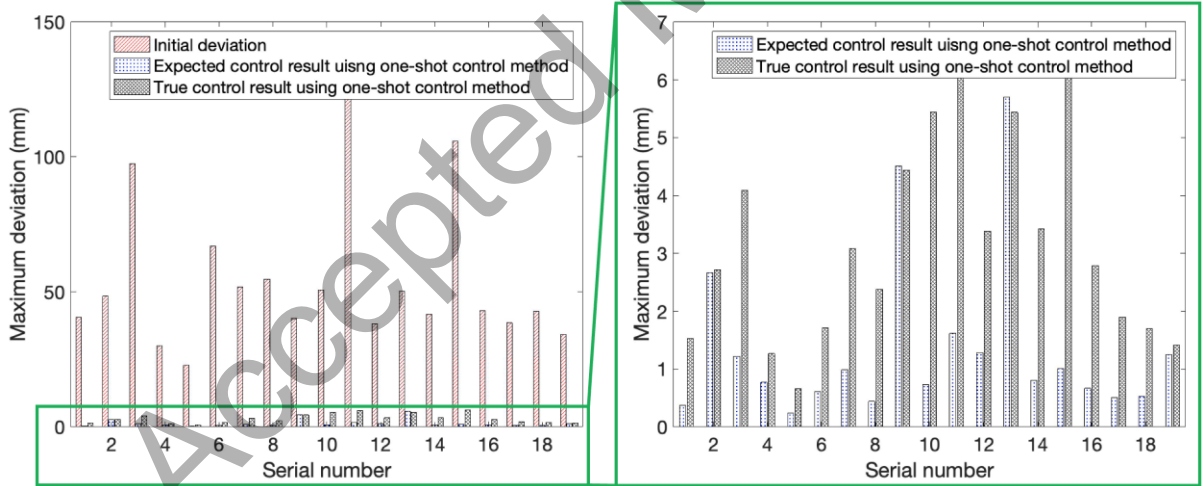

Figure 4. Comparison among the initial deviation, expected control result, and true control result

In Figure 4, the x-axis represents the fuselage serial number, and the y-axis is the maximum deviation. We can see that even though the one-shot control strategy reduces the deviation significantly, in most cases, the real control performance is far worse than the expected one. This is due to the fact that the control law derived based on the FEA-based model for the designed shape is

not optimal for the incoming fuselage with specific dimensional errors and material properties characteristics. They may perform well on the ideal fuselage, but the control performance on a specific incoming fuselage with initial deviation is not guaranteed. The large discrepancy between the true control performance and the expected control performance indicates the necessity of adopting the adaptive control method.

To evaluate the adaptive control performance, 100 simulations are conducted for each fuselage. In each simulation, we first randomly generate actuator forces as the input to FEA software and record the corresponding shape deviation. Then an i.i.d. Gaussian random noise with mean zeros and standard deviation 0.066 mm will be added to each node on top of the shape deviation as the measured response signal to mimic the measurement error. We repeat this process 100 times and get 100 pairs of actuator's forces and response to estimate **A**. Finally, the control strategy is derived by solving Equation (12). The median and 3σ limit of control performance is reported in Figure 5. In Figure 5, the fuselage serial number is shown on the x-axis, and the y-axis represents the maximum deviation. The right-slanted bar is the control performance using the one-shot control method, and the crossed bar with the 3-sigma error bound shows the performance of using the adaptive control method. We use the average percentage of performance improvement (APPI) as the evaluation criterion, i.e.,

$$APPI = \frac{1}{19} \sum_{i=1}^{19} \frac{\left(d_{b_i} - d_{a_i}\right)}{d_{b_i}} \times 100\%,$$

where d_{b_i} and d_{a_i} are the maximum deviations of two control methods to be compared, i.e., d_{b_i} is the maximum shape deviation of the ith fuselage by applying the one-shot control method and d_{a_i} is the maximum shape deviation of the ith fuselage after applying the proposed control method. The APPI evaluates the performance improvement of the proposed control method over the benchmark one-shot control method. The larger the APPI value indicates a better control performance. On average, the performance improvement is 54.31%. Note that when the expected and true control results are close, i.e., No.2, No.9, and No.13, the adaptive control does not improve the control result significantly. This is because when the process variability is low, the incoming fuselages can be represented very

17

accurately with the FEA-based model, and perturbations to the system equation have a slight and neglectable influence. According to Proposition 2, we can calculate the predicted adaptive control result (set **C** as the identity matrix), which is the dotted bar in Figure 5. We can see that the predicted result matches the experiment result.
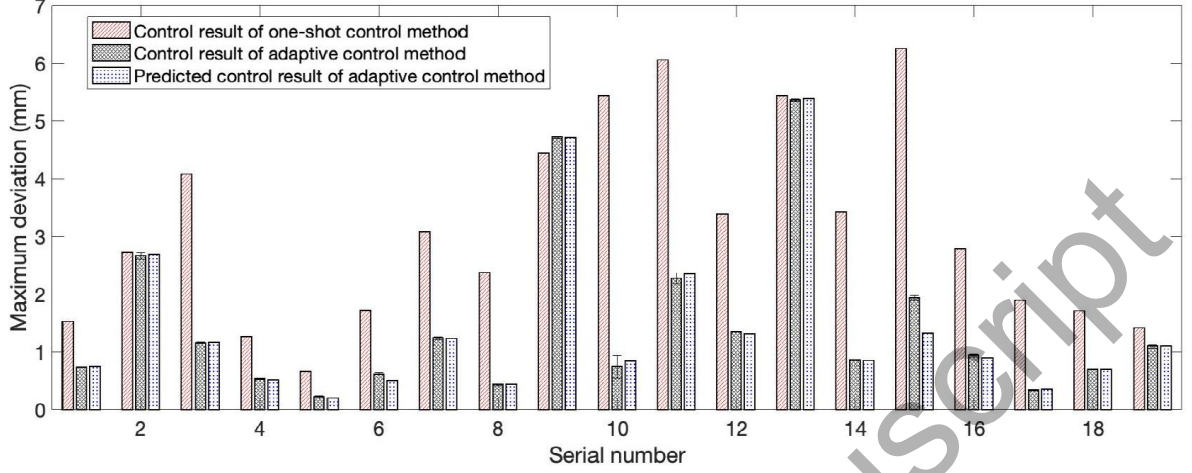

Figure 5. Comparison of the control performance between one-shot control and adaptive control

As we mentioned in Section 3.2, measuring every point is an expensive and challenging task when considering the sensing budget. Since the change of response signal y, due to control actions, lives in a much lower-dimensional space, sparse sensor placement is a viable alternative. However, the lower-dimensional space is unknown due to the unknown matrix **A**. In the next section, we will show that, under small perturbations, the proposed method can still achieve satisfactory performance even using $\mathbf{A}_0$ (the design information) to develop a sensing strategy and reconstruct the entire response signal.

3.3   *Control performance of SPAC strategy*

In this section, the sparse learning method (Du et al. 2019) is applied to 19 fuselages with the same tuning parameters. Then, the proposed SPAC strategy is adopted to further control the fuselage to its target shape. For each fuselage, we assume that the sensor budget is restricted to 20, which means we should use at most 20 sensor measurements to reconstruct the 186-dimensional response. The determinant criterion is adopted, and the QR pivoting algorithm (Manohar et al. 2018a) is used to

18

select sensor locations. The selected sensor locations are shown as solid points in Figure 6. Notice that the sensor locations are selected according to the designed matrix $\mathbf{A}_0$, which is the same for all 19 fuselages. Therefore, the selected sensor locations are the same among these 19 fuselages.
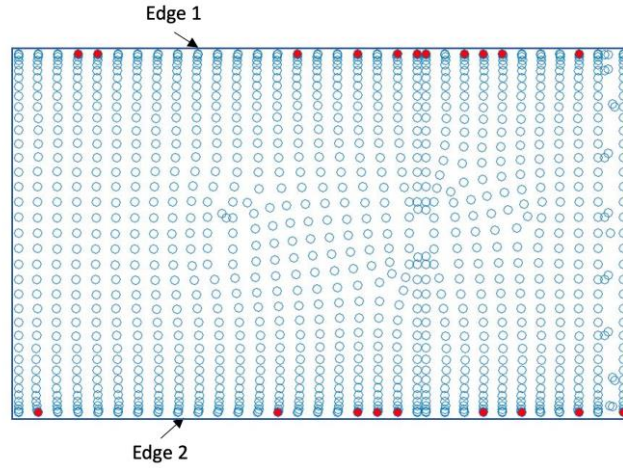

Figure 6. Selected sensor locations

The control result is shown in Figure 7. The right-slanted bar is the one-shot control result; the crossed bar is the adaptive control result when all points are measured (186 dimensional), and the left-slanted bar is the SPAC result with only 20-dimensional measurement. According to Proposition 2, we can calculate the predicted SPAC control result which is the dotted bar. We can see that the predicted result matches the experiment result. By adopting the SPAC method, the one-shot control performance is improved by 53.93%. It can achieve comparable control results with the adaptive control method but only measures less than 11% of the full response signal. This can significantly reduce the sensing cost.
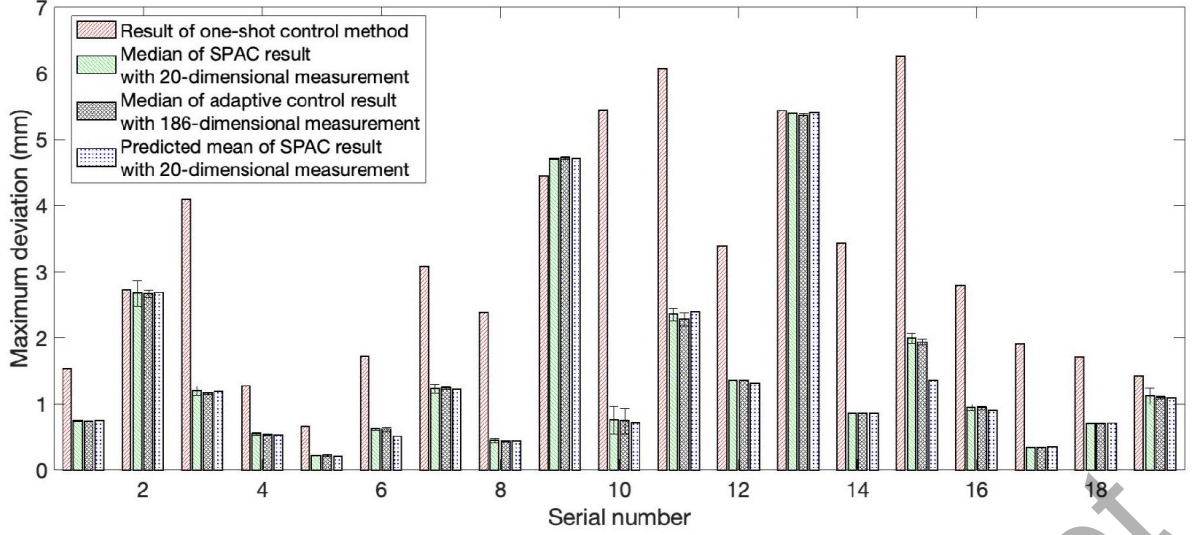
Figure 7. Comparison among the one-shot control, the adaptive control with 186-dimensional

measurement, and the SPAC with 20-dimensional measurement

We conduct a sensitivity analysis by varying the number of sensors from 5 to 180 with the interval 5 and recording the corresponding control performance. The result is shown in Figure 8. The x-axis represents the number of sensors used for measurement and the y-axis represents the APPI value. The solid curve demonstrates the APPI of adaptive control result with 186-dimensional measurement and the dashed curve demonstrates the APPI of the SPAC method. We can see that after the number of sensors reaches 20, the control performance of the SPAC method approaches the adaptive control result with 186-dimensional measurement. The control performance improvement of further increasing the number of sensors is not significant. This demonstrates the effectiveness of the proposed SPAC method. Notice that the APPI of the proposed SPAC method is unstable when the number of sensors is less than 20. This is because the number of sensors is less than the dimension of the subspace where the signal exists, which will lead to a suboptimal reconstruction performance and deteriorate the control performance.
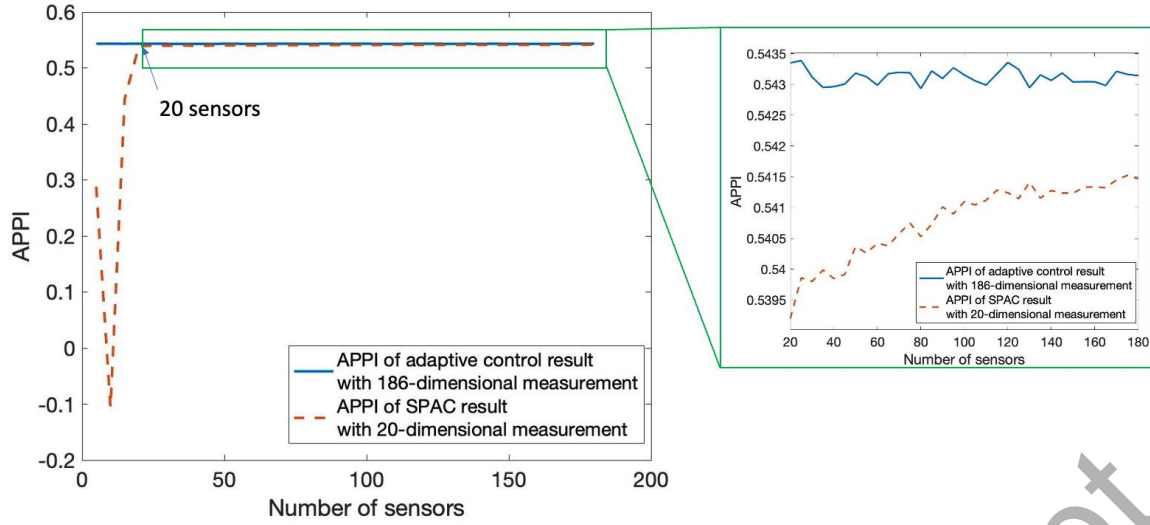
Figure 8. Sensitivity analysis of the SPAC method by varying the number of sensors

4. Conclusion

High-dimensional systems with variability are common in many engineering applications due to inherent process variations. This paper proposes a SPAC method for perturbed high-dimensional systems to reduce the sensing cost and optimize the control performance. We formalize and analyze a sparse optimization framework for the sparse placement of measurement sensors and incorporate it into the adaptive control framework. We first establish the relationship between the reconstruction performance and the corresponding perturbation level. An analytical bound, as well as its engineering interpretation, are derived. An adaptive control strategy based on the sparse measurement is proposed, whose performance is validated using a case study from a high precision fuselage assembly process.

The proposed method provides a holistic approach to make use of the feedback information for parameter estimation and control under sparse sensor placement strategies. By incorporating the designed system information, a significant reduction in sensing cost can be achieved while maintaining comparable control performance. One possible future research direction is to consider the trade-off between the number of sensors and the control performance to optimize the control and sensing cost. Another possible research direction is to study the performance of the SPAC strategy when the plant settings vary slowly over time.

21

Acknowledgment

Data and Code Availability Statement

The code is available via the link: https://github.com/Shancong-Mou/SPAC.

References

Åström, K. J. (1983). "Theory and applications of adaptive control—a survey." *Automatica* **19**(5): 471-486.

Åström, K. J. and B. Wittenmark (2013). *Adaptive Control*, second edition, Courier Corporation, North Chelmsford, MA, USA.

Bhattacharya, S. and T. Başar (2011). Sparsity based feedback design: A new paradigm in opportunistic sensing. in *Proceedings of the 2011 American Control Conference*, IEEE, San Francisco, CA, USA, pp. 3704-3709, doi: 10.1109/ACC.2011.5991014.

Brunton, B. W., S. L. Brunton, J. L. Proctor and J. N. Kutz (2016). "Sparse sensor placement optimization for classification." *SIAM Journal on Applied Mathematics* **76**(5): 2099-2122.

Candès, E. J. and M. B. Wakin (2008). "An introduction to compressive sampling." *IEEE Signal Processing Magazine* **25**(2): 21-30.

Chaloner, K. and I. Verdinelli (1995). "Bayesian experimental design: A review." *Statistical Science* **10**(3): 273-304.

Clyne, T. W. and D. Hull (2019). *An introduction to composite materials*, Cambridge university press, Cambridge, UK.

Donoho, D. L. (2006). "Compressed Sensing." *IEEE Transactions on Information Theory* **52**(4): 1289-1306.

Du, J., X. Yue, J. H. Hunt and J. Shi (2019). "Optimal placement of actuators via sparse learning for composite fuselage shape control." *ASME Transactions, Journal of Manufacturing Science and Engineering* **141**(10): 101004.

Duncan, I. (2021). "Boeing discloses manufacturing problem with 787 Dreamliner that it says will slow production of jets." *The Washington Post.* (Retrieved April 23, 2022, from https://www.washingtonpost.com/transportation/2021/07/13/boeing-787-dreamliner-problem/).

Joshi, S. and S. Boyd (2008). "Sensor selection via convex optimization." *IEEE Transactions on Signal Processing* **57**(2): 451-462.

Kramer, B., P. Grover, P. Boufounos, S. Nabi and M. Benosman (2017). "Sparse sensing and DMD-based identification of flow regimes and bifurcations in complex flows." *SIAM Journal on Applied Dynamical Systems* **16**(2): 1164-1196.

Landau, I. D., R. Lozano, M. M'Saad and A. Karimi (2011). *Adaptive Control: Algorithms, Analysis and Applications*, Springer Science & Business Media, New York, NY, USA.

Lee, C., J. Wu, W. Wang and X. Yue (2022), "Neural Network Gaussian Process Considering Input Uncertainty for Composite Structure Assembly," *IEEE/ASME Transactions on Mechatronics*, **27**(3): 1267-1277, doi: 10.1109/TMECH.2020.3040755.

Manohar, K., B. W. Brunton, J. N. Kutz and S. L. Brunton (2018a). "Data-driven sparse sensor placement for reconstruction: Demonstrating the benefits of exploiting known patterns." *IEEE Control Systems Magazine* **38**(3): 63-86.

Manohar, K., T. Hogan, J. Buttrick, A. G. Banerjee, J. N. Kutz and S. L. Brunton (2018b). "Predicting shim gaps in aircraft assembly with machine learning and sparse sensing." *Journal of Manufacturing Systems* **48**: 87-95.

Mei, Z. and P. G. Maropoulos (2014). "Review of the application of flexible, measurement-assisted assembly technology in aircraft manufacturing." *Proceedings of the Institution of Mechanical Engineers, Part B: Journal of Engineering Manufacture* **228**(10): 1185-1197.

Meo, M. and G. Zumpano (2005). "On the optimal sensor placement techniques for a bridge structure." *Engineering Structures* **27**(10): 1488-1497.

Muralikrishnan, B., S. Phillips and D. Sawyer (2016). "Laser trackers for large-scale dimensional metrology: A review." *Precision Engineering* **44**: 13-28.

Reddy, J. N. (2019). *Introduction to the Finite Element Method*, McGraw-Hill Education, New York, NY, USA.

Sloan, J. (2018). "The first composite fuselage section for the first composite commercial jet." *Composites World*. Available at https://www.compositesworld.com/articles/the-first-composite-fuselage-section-for-the-first-composite-commercial-jet, (accessed 15 December 2021).

Wang, W., X. Yue, B. Haaland, and Jeff C.F. Wu (2022). "Gaussian processes with input location error and applications to the composite parts assembly process." *SIAM/ASA Journal on Uncertainty Quantification*, **10**(2), 619-650.

Wen, Y., X. Yue, J. H. Hunt and J. Shi (2018). "Feasibility analysis of composite fuselage shape control via finite element analysis." *Journal of Manufacturing Systems* **46**: 272-281.

Yang, X., D. Venturi, C. Chen, C. Chryssostomidis and G. E. Karniadakis (2010). "EOF‐based constrained sensor placement and field reconstruction from noisy ocean measurements: Application to Nantucket Sound." *Journal of Geophysical Research: Oceans* **115**(C12).

Yue, X., Y. Wen, J. H. Hunt and J. Shi (2018). "Surrogate model-based control considering uncertainties for composite fuselage assembly." *ASME Transactions, Journal of Manufacturing Science and Engineering* **140**(4): 041017.

Yue, X. and Shi, J., 2018. Surrogate model–based optimal feed-forward control for dimensional-variation reduction in composite parts' assembly processes. *Journal of Quality Technology*, **50**(3), pp.279-289.

Zhang, T. and J. Shi (2016a). "Stream of variation modeling and analysis for compliant composite part assembly—part I: single-station processes." *ASME Transactions, Journal of Manufacturing Science and Engineering* **138**(12): 121003.

Zhang, T. and J. Shi (2016b). "Stream of variation modeling and analysis for compliant composite part assembly—Part II: Multistation processes." *ASME Transactions, Journal of Manufacturing Science and Engineering* **138**(12): 121004.

Zhong, Z., S. Mou, J. H. Hunt and J. Shi (2021). "FEA model based cautious automatic optimal shape control for fuselage assembly." *ASME Transactions, Journal of Manufacturing Science and Engineering* **144**(8): 081009.

Shancong Mou
H. Milton Stewart School of Industrial and Systems Engineering,
Georgia Institute of Technology,
Atlanta, GA 30332
e-mail: shancong.mou@gatech.edu

Shancong Mou received the B.S. degree in energy and power engineering from Xi'an Jiaotong University, Xi'an, China, in 2017. He is currently pursuing the Ph.D. degree with the School of Industrial and Systems Engineering, Georgia Tech, Atlanta, GA, USA. His research interests include data analytics for monitoring, control, and diagnostics of complex engineering systems. Mr. Mou is also a member of the Institute of Industrial and Systems Engineers (IISE) and the Institute for Operations Research and the Management Sciences (INFORMS).

Xiaowei Yue*
Grado Department of Industrial and Systems Engineering,
Virginia Polytechnic Institute and State University,
Blacksburg, VA 24061
e-mail: xwy@vt.edu

Dr. Xiaowei Yue got his Ph.D. degree in Industrial Engineering, M.S. in Statistics from Georgia Tech, M.S. in Power Engineering and Thermophysics from Tsinghua University, B.S. in Mechanical Engineering from BIT. Currently, He is an assistant professor at the Grado Department of Industrial and Systems Engineering, Virginia Tech. His research interests focus on data analytics and quality control for advanced manufacturing. He is a recipient of Outstanding Young Manufacturing Engineer Award from SME. Dr. Yue serves as an associate editor for the IISE Transactions and the Journal of Intelligent Manufacturing. Dr. Yue is a senior member of IISE, ASQ and IEEE.

Michael Biehler
H. Milton Stewart School of Industrial and Systems Engineering,
Georgia Institute of Technology,
Atlanta, GA 30332
e-mail: michael.biehler@gatech.edu

Michael Biehler received his B.S. and M.S in Industrial and Mechanical Engineering from Karlsruhe Institute of Technology (KIT)in 2017 and 2020, respectively. Currently, he is a Ph.D. candidate in the H. Milton Stewart School of Industrial and Systems Engineering, Georgia Institute of Technology. His research rests at the interface between machine learning and cyber-physical (manufacturing) systems, where he aims to develop methods for cyber security and 3D machine learning, system monitoring, and control.

Jeffrey H. Hunt
The Boeing Company,
900 N Sepulveda Blvd, El Segundo, CA 90245
e-mail: jeffrey.h.hunt@boeing.com

Dr. Jeffrey H. Hunt received the B.S. degree in physics from the Massachusetts Institute of Technology, Cambridge, MA, USA, in 1979, and the M.A. degree in physics and the Ph.D. degree in physics from the University of California at Berkeley, Berkeley, CA, USA, in 1981 and 1988, respectively. He is currently a Principal Scientist and a Senior Technical Fellow with Boeing Company, El Segundo, CA, USA. His career has included physics-based projects in condensed matter physics, quantum information sciences, surface science, and nonlinear optics and work on diverse applications, including both in defense sciences and commercial air and space technologies. He has published over 30 articles, three books, and two encyclopedia articles on condensed matter sciences. He holds 61 U.S. patents. His main research areas are wide scientific and technical challenges in

aviation and aerospace industry, with particular applications in condensed matter sciences and nonlinear optics, composite aircraft assembly, and so on. Dr. Hunt is a fellow of the American Physical Society and the Optical Society of America.

Jianjun Shi
Fellow IISE
H. Milton Stewart School of Industrial and Systems Engineering,
Georgia Institute of Technology,
Atlanta, GA 30332
e-mail: jianjun.shi@isye.gatech.edu

Dr. Jianjun Shi (https://sites.gatech.edu/jianjun-shi/) received the B.S. and M.S. degrees in automation from the Beijing Institute of Technology in 1984 and 1987, respectively, and the Ph.D. degree in mechanical engineering from the University of Michigan in 1992. Currently, Dr. Shi is the Carolyn J. Stewart Chair and Professor at the Stewart School of Industrial and Systems Engineering, Georgia Institute of Technology. His research interests include the fusion of advanced statistical and domain knowledge to develop methodologies for modeling, monitoring, diagnosis, and control for complex manufacturing systems. Dr. Shi is a Fellow of four professional societies, including ASME, IISE, INFORMS, and SME, an elected member of the International Statistics Institute (ISI), a life member of ASA, an Academician of the International Academy for Quality (IAQ), and a member of National Academy of Engineers (NAE).